PERGAMON

International Journal of Solids and Structures 36 (1999) 3483–3496

INTERNATIONAL JOURNAL OF SOLIDS and STRUCTURES

Dynamic stability of cylindrical panels with transverse shear effects

T. Y. Ng[a,*], K. Y. Lam[a], J. N. Reddy[b]

[a] *Department of Mechanical and Production Engineering, National University of Singapore, 10 Kent Ridge Crescent, Singapore 119260*

[b] *Department of Mechanical Engineering, Texas A&M University, College Station, TX 77843–3123, U.S.A.*

Received 10 October 1997; in revised form 18 May 1998

Abstract

The dynamic stability of simply-supported, isotropic cylindrical panels under combined static and periodic axial forces are investigated. An extension of Donnell's shell theory to a first-order shear deformation theory is used, and a system of Mathieu–Hill equations are obtained via a normal-mode expansion, and the parametric resonance response was analyzed using Bolotin's method. Results are compared with those obtained using the classical shell theory. The effects of the thickness-to-radius ratio on the instability regions are examined in detail.

1. Introduction

The static and dynamic analysis of shells have been studied for a long time. Among the well-known shells theories are: Donnell's (1933) theory, Love's (1944) theory, Flugge's (1962) theory and Sander's theory (1959). The study of thin cylindrical panels usually involve the use of these theories with emphasis on the development of solution methods. The methods of solution are mostly exact closed-form solutions, Webster (1968), Blevins (1981) and Soldatos and Hadjigeoriou (1990), or series analytical solutions, Leissa et al. (1981), Koumousis and Armenakas (1984) and Palazotto and Linnemann (1991). To cater for moderately thick shells, the effects of transverse shear deformation and rotary inertias were first considered by Gulati and Essenberg (1967) and Zukas and Vinson (1971). Exact solutions were later presented by Bert and Chen (1978), Bert and Kumar (1982) and Reddy (1984) for the critical buckling and free vibration of moderately thick laminated plates and shells. More recent works regarding this subject include those by Muc (1989), Moorthy et al. (1990), Carrera (1991), Nosier and Reddy (1992) and Reddy (1996).

Structural components under periodic loads can undergo parametric resonance which may occur

* Corresponding author. Fax: 00 65 775 0092; E-mail: ngty@ihpc.nus.edu.sg

0020–7683/99/$ - see front matter
PII: S0020–7683(98)00161–9

over a range of forcing frequencies and has become a popular subject of study. It was first examined by Bolotin (1964), Yao (1965) and Vijayaraghavan and Evan-Iwanowski (1967). For thin cylindrical shells under periodic axial loads, the method of solution is almost always to first reduce the equations of motion to a system of Mathieu–Hill equations. The dynamic stability for such a system of equations can then be analyzed by a number of methods. For direct parametric resonances, the simple and well-known method due to Bolotin (1964) reduces the system of Mathieu–Hill equations to the standard form of a generalized eigenvalue problem where solutions are easily computed. A literature search showed that studies comparing the instability regions generated using classical shell theory (CST) and first-order shear deformation theory (FSDT) are not available. Such a study would be interesting and useful as it would shed light on the relative importance of the inclusion of shear deformation and rotary inertia effects when predicting the widths of the unstable regions.

In the present analysis, the dynamic stability of isotropic cylindrical panels under combined static and periodic axial forces is studied using an extension of Donnell's shell theory to a first-order shear deformation theory. The results obtained were compared with those obtained using classical shell theory. The method of solution is such that a normal-mode expansion of the equations of motion yield a system of Mathieu–Hill equations and the parametric resonance responses are analyzed based on Bolotin's method. The present formulation of the problem is also made general to accommodate any boundary conditions but for reasons of simplicity, the comparison study is only carried out for the case of simply-supported boundary conditions.

2. Theory and formulation

The cylindrical panel as shown in Fig. 1 is assumed to be thin and of uniform thickness. It is of length L, radius R, thickness h, width b and shallowness angle α. The x-axis is taken along a generator, the circumferential arc length subtends an angle θ, and the z-axis is directed radially inwards. The panel is isotropic with elastic modulus E, Poisson's ratio v and material mass density ρ. The pulsating extensional axial load is given by

$$N_a(x,t) = N_0 + N_s \cos Pt \tag{1}$$

where P is the frequency of excitation in radians per unit time.

In the present analysis, the equations of motion with first-order shear deformation theory (FSDT) of a cylindrical panel using Donnell's theory as presented in Nosier and Reddy (1992) are

$$\begin{aligned}
&\frac{\partial N_1}{\partial x} + \frac{1}{R}\frac{\partial N_6}{\partial \theta} = I_1\ddot{u} + I_2\ddot{\phi}_1, \quad \frac{\partial N_6}{\partial x} + \frac{1}{R}\frac{\partial N_2}{\partial \theta} = I_1\ddot{v} + I_2\ddot{\phi}_2,\\
&\frac{\partial M_1}{\partial x} + \frac{1}{R}\frac{\partial M_6}{\partial \theta} - Q_1 = I_2\ddot{u} + I_3\ddot{\phi}_1, \quad \frac{\partial M_6}{\partial x} + \frac{1}{R}\frac{\partial M_2}{\partial \theta} - Q_2 = I_2\ddot{v} + I_3\ddot{\phi}_2,\\
&\frac{\partial Q_1}{\partial x} + \frac{1}{R}\frac{\partial Q_2}{\partial \theta} - \frac{N_2}{R} + \frac{\partial}{\partial x}\left(N_a\frac{\partial w}{\partial x}\right) = I_1\ddot{w},
\end{aligned} \tag{2}$$

where u, v and w are the displacement components in the x, y and z directions (see Fig. 1) and ϕ_1

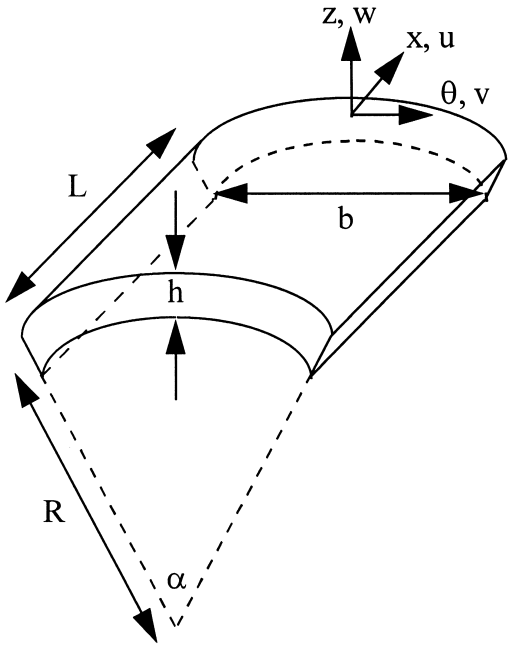

Fig. 1. Coordinate system of the cylindrical panel.

and ϕ_2 are the rotation functions. A superposed dot indicates differentiation with respect to time t. For an isotropic cylindrical panel, the stress resultants are

$$\begin{aligned} N_1 &= A_{11}\varepsilon_1 + A_{12}\varepsilon_2, & N_2 &= A_{21}\varepsilon_1 + A_{22}\varepsilon_2, \\ M_1 &= D_{11}\kappa_1 + D_{12}\kappa_2, & M_2 &= D_{21}\kappa_1 + D_{22}\kappa_2, \\ N_6 &= A_{66}\varepsilon_6, & M_6 &= D_{66}\kappa_6, \\ Q_1 &= k_5 A_{55}\varepsilon_5, & Q_2 &= k_4 A_{44}\varepsilon_4, \end{aligned} \tag{3}$$

where k_4 and k_5 are the shear correction factors and the stiffnesses $A_{i,j}$, $B_{i,j}$ and $D_{i,j}$ are defined as

$$A_{11} = A_{22} = \frac{Eh}{1-v^2}, \quad A_{12} = A_{21} = v\frac{Eh}{1-v^2}, \quad A_{44} = A_{55} = A_{66} = \frac{Eh}{2(1+v)},$$

$$D_{11} = D_{22} = \frac{Eh^3}{12(1-v^2)}, \quad D_{12} = D_{21} = v\frac{Eh^3}{12(1-v^2)}, \quad D_{66} = \frac{Eh^3}{24(1+v),} \tag{4}$$

and the mass terms and strain and curvature expressions of eqns (2) and (3) are defined as

$$(I_1, I_2, I_3) = \int_{-h/2}^{h/2} \rho(1, z, z^2)\,\mathrm{d}z \tag{5}$$

$$\varepsilon_1 = \frac{\partial u}{\partial x}, \quad \varepsilon_2 = \frac{1}{R}\left(\frac{\partial v}{\partial \theta} + w\right), \quad \varepsilon_4 = \phi_2 + \frac{1}{R}\frac{\partial w}{\partial \theta},$$

$$\varepsilon_5 = \phi_1 + \frac{\partial w}{\partial x}, \quad \varepsilon_6 = \frac{\partial w}{\partial x} + \frac{1}{R}\frac{\partial u}{\partial \theta},$$

$$\kappa_1 = \frac{\partial \phi_1}{\partial x}, \quad \kappa_2 = \frac{1}{R}\frac{\partial \phi_2}{\partial \theta}, \quad \kappa_6 = \frac{\partial \phi_2}{\partial x} + \frac{1}{R}\frac{\partial \phi_1}{\partial \theta}. \tag{6}$$

The equations of motion of the classical shell theory (CST) are obtained from eqn (1) by neglecting terms involving I_1 and I_2 and by setting

$$\phi_1 = -\frac{\partial w}{\partial x}, \quad \phi_2 = -\frac{\partial w}{\partial \theta}. \tag{7}$$

If the panel is simply-supported along all the edges, there exists a solution for the equations of motion in the form

$$u_{mn} = A_{mn}\, e^{i\omega t} \cos\frac{m\pi x}{L} \sin\frac{n\pi\theta}{\alpha}$$

$$v_{mn} = B_{mn}\, e^{i\omega t} \sin\frac{m\pi x}{L} \cos\frac{n\pi\theta}{\alpha}$$

$$\phi_{1_{mn}} = \frac{C_{mn}}{R} e^{i\omega t} \cos\frac{m\pi x}{L} \sin\frac{n\pi\theta}{\alpha}$$

$$\phi_{2_{mn}} = \frac{D_{mn}}{R} e^{i\omega t} \sin\frac{m\pi x}{L} \cos\frac{n\pi\theta}{\alpha}$$

$$w_{mn} = F_{mn}\, e^{i\omega t} \sin\frac{m\pi x}{L} \sin\frac{n\pi\theta}{\alpha} \tag{8}$$

where n represents the number of circumferential waves and m the number of axial half-waves in the corresponding standing wave pattern.

The non-dimensional pulsating axial load parameter η is given by

$$\eta = \frac{N(1-\nu^2)}{Eh}. \tag{9}$$

Thus eqn (1) can be written as

$$\eta_a = \eta_0 + \eta_s \cos Pt. \tag{10}$$

The equations of motion can be solved using an eigenfunction expansion in terms of the normal modes of the free vibrations of a cylindrical panel under a constant axial load η_0 with the oscillating component $\eta_s = 0$. Substitution of eqn (6) into the equations of motion which are a set of five coupled homogeneous equations yields a 5×5 frequency equation when the determinant is equated

to zero. Thus, for each m and n, there exists five roots corresponding to the transverse, axial, circumferential modes and two rotational modes.

To solve the equations of motion that include the oscillating component η_s, a solution is sought in the form shown below where all the modes are superimposed,

$$u_{mnj} = \sum_{j=1}^{5}\sum_{m=1}^{\infty}\sum_{n=1}^{\infty} A_{mnj}q_{mnj}(t)\cos\lambda x\sin\mu\theta$$

$$v_{mnj} = \sum_{j=1}^{5}\sum_{m=1}^{\infty}\sum_{n=1}^{\infty} B_{mnj}q_{mnj}(t)\sin\lambda x\cos\mu\theta$$

$$\phi_{1_{mnj}} = \sum_{j=1}^{5}\sum_{m=1}^{\infty}\sum_{n=1}^{\infty} \frac{C_{mnj}}{R}q_{mnj}(t)\cos\lambda x\sin\mu\theta$$

$$\phi_{2_{mnj}} = \sum_{j=}^{5}\sum_{m=1}^{\infty}\sum_{n=1}^{\infty} \frac{D_{mnj}}{R}qq_{mnj}(t)\sin\lambda x\cos\mu\theta$$

$$w_{mnj} = \sum_{j=1}^{5}\sum_{m=1}^{\infty}\sum_{n=1}^{\infty} F_{mnj}q_{mnj}(t)\sin\lambda x\sin\mu\theta \tag{11}$$

where $q_{mnj}(t)$ is a generalized coordinate and

$$\lambda = \frac{m\pi}{L}, \quad \mu = \frac{n\pi}{\alpha}. \tag{12}$$

Substituting eqn (11) into the equations of motion and simplifying yields

$$\sum_{j=1}^{5}\sum_{m=1}^{\infty}\sum_{n=1}^{\infty}(\ddot{q}_{mnj}+\omega_{mnj}^2q_{mnj})\gamma\left(\bar{A}_{mnj}I_1+\frac{I_2}{R}\bar{C}_{mnj}\right)\cos\lambda x\sin\mu\theta = 0 \tag{13}$$

$$\sum_{j=1}^{5}\sum_{m=1}^{\infty}\sum_{n=1}^{\infty}(\ddot{q}_{mnj}+\omega_{mnj}^2q_{mnj})\gamma\left(\bar{B}_{mnj}I_1+\frac{I_2}{R}\bar{D}_{mnj}\right)\sin\lambda x\cos\mu\theta = 0 \tag{14}$$

$$\sum_{j=1}^{5}\sum_{m=1}^{\infty}\sum_{n=1}^{\infty}(\ddot{q}_{mnj}+\omega_{mnj}^2q_{mnj})\frac{\gamma}{R}\left(\bar{A}_{mnj}I_2+\frac{I_3}{R}\bar{C}_{mnj}\right)\cos\lambda x\sin\mu\theta = 0 \tag{15}$$

$$\sum_{j=1}^{5}\sum_{m=1}^{\infty}\sum_{n=1}^{\infty}(\ddot{q}_{mnj}+\omega_{mnj}^2q_{mnj})\frac{\gamma}{R}\left(\bar{B}_{mnj}I_2+\frac{I_3}{R}\bar{D}_{mnj}\right)\sin\lambda x\cos\mu\theta = 0 \tag{16}$$

$$\sum_{j=1}^{5}\sum_{m=1}^{\infty}\sum_{n=1}^{\infty}(\ddot{q}_{mnj}+\omega_{mnj}^2q_{mnj})\gamma I_1\sin\lambda x\sin\mu\theta$$
$$+R^2\lambda\cos Pt\sum_{j=1}^{5}\sum_{m=1}^{\infty}\sum_{n=1}^{\infty}q_{mnj}\frac{\partial}{\partial x}(\eta_s\cos\lambda x)\sin\mu\theta = 0 \tag{17}$$

where

$$\gamma = \frac{R^2(1-v^2)}{Eh} \tag{18}$$

and

$$\bar{A}_{mnj} = \frac{A_{mnj}}{F_{mnj}}, \quad \bar{B}_{mnj} = \frac{B_{mnj}}{F_{mnj}}, \quad \bar{C}_{mnj} = \frac{C_{mnj}}{F_{mnj}}, \quad \bar{D}_{mnj} = \frac{D_{mnj}}{F_{mnj}}. \tag{19}$$

Making use of the orthogonality condition, we multiply eqn (13) by $\gamma(\bar{A}_{rsi}I_1 + (I_2/R)\bar{C}_{rsi})\cos\lambda_r x \sin\mu_s\theta$, eqn (14) by $\gamma(\bar{B}_{rsi}I_1 + (I_2/R)\bar{D}_{rsi})\sin\lambda_r x\cos\mu_s\theta$, eqn (15) by $(\gamma/\mathrm{R})(\bar{A}_{rsi}I_2 + (I_3/R)\bar{C}_{rsi})\cos\lambda_r x \sin\mu_s\theta$, eqn (16) by $(\gamma/R)(\bar{B}_{rsi}I_2 + (I_3/R)\bar{D}_{rsi})\sin\lambda_r x\cos\mu_s\theta$ and eqn (17) by $\gamma I_1 \sin\lambda_r x \sin\mu_s\theta$. We then add the five resulting equations and integrate over the surface of the panel. This yields the following set of equations

$$\mathbf{M}_{IJ}\ddot{\mathbf{q}}_J + (\mathbf{K}_{IJ} - \cos Pt\mathbf{Q}_{IJ})\mathbf{q}_J = 0 \tag{20}$$

where $\mathbf{M}_{IJ}$, $\mathbf{K}_{IJ}$ and $\mathbf{Q}_{IJ}$ are matrices and $\ddot{\mathbf{q}}_J$ and $\mathbf{q}_J$ are column vectors consisting of $\ddot{q}_{mnj}$ and q_{mnj}, respectively, and

$$\begin{aligned}
r &= 1,2,3,4,\ldots,N\\
s &= 1,2,3,4,\ldots,N\\
i &= 1,2,3,4,5\\
m &= 1,2,3,4,\ldots,N\\
n &= 1,2,3,4,\ldots,N\\
j &= 1,2,3,4,5\\
I &= 1,2,3,4,\ldots,(N\times N\times 5)\\
J &= 1,2,3,4,\ldots,(N\times N\times 5)
\end{aligned} \tag{21}$$

where for

$$\begin{aligned}
I = 1, &\quad r = 1 \quad s = 1 \quad i = 1\\
I = 2, &\quad r = 1 \quad s = 1 \quad i = 2\\
I = 3, &\quad r = 1 \quad s = 1 \quad i = 3\\
I = 4, &\quad r = 1 \quad s = 1 \quad i = 4\\
I = 5, &\quad r = 1 \quad s = 1 \quad i = 5\\
I = 6, &\quad r = 1 \quad s = 2 \quad i = 1\\
I = 7, &\quad r = 1 \quad s = 2 \quad i = 2\\
I = 8, &\quad r = 1 \quad s = 2 \quad i = 3\\
I = 9, &\quad r = 1 \quad s = 2 \quad i = 4
\end{aligned}$$

$$
\begin{aligned}
&I = 10, \quad r = 1 \quad s = 2 \quad i = 5\\
&\quad\vdots\\
&I = 5N-4, \quad r = 1 \quad s = N \quad i = 1\\
&I = 5N-3, \quad r = 1 \quad s = N \quad i = 2\\
&I = 5N-2, \quad r = 1 \quad s = N \quad i = 3\\
&I = 5N-1, \quad r = 1 \quad s = N \quad i = 4\\
&I = 5N, \qquad r = 1 \quad s = N \quad i = 5\\
&I = 5N+1, \quad r = 2 \quad s = 1 \quad i = 1\\
&I = 5N+2, \quad r = 2 \quad s = 1 \quad i = 2\\
&I = 5N+3, \quad r = 2 \quad s = 1 \quad i = 3\\
&I = 5N+4, \quad r = 2 \quad s = 1 \quad i = 4\\
&I = 5N+5, \quad r = 2 \quad s = 1 \quad i = 5\\
&\quad\vdots\\
&I = 5N^2-4, \quad r = N \quad s = N \quad i = 1\\
&I = 5N^2-3, \quad r = N \quad s = N \quad i = 2\\
&I = 5N^2-2, \quad r = N \quad s = N \quad i = 3\\
&I = 5N^2-1, \quad r = N \quad s = N \quad i = 4\\
&I = 5N^2, \qquad r = N \quad s = N \quad i = 5.
\end{aligned}
\tag{22}
$$

The co-relations between the subscripts, J, m, n and j follow that of I, r, s and i, respectively. The matrices $\mathbf{M}_{IJ}$, $\mathbf{K}_{IJ}$ and $\mathbf{Q}_{IJ}$ are given as

$$
\begin{aligned}
\bar{\mathbf{M}}_{IJ} = \int_0^L \int_0^\alpha \Bigg\{ & \gamma^2 \left(\bar{A}_I I_1 + \frac{I_2}{R}\bar{C}_I\right)\left(\bar{A}_J I_1 + \frac{I_2}{R}\bar{C}_J\right)\cos\lambda_r x \sin\mu_s\theta \cos\lambda_m x \sin\mu_n\theta\\
& + \gamma^2 \left(\bar{B}_I I_1 + \frac{I_2}{R}\bar{D}_I\right)\left(\bar{B}_J I_1 + \frac{I_2}{R}\bar{D}_J\right)\sin\lambda_r x \cos\mu_s\theta \sin\lambda_m x \cos\mu_n\theta\\
& + \left(\frac{\gamma}{R}\right)^2 \left(\bar{A}_I I_2 + \frac{I_3}{R}\bar{C}_I\right)\left(\bar{A}_J I_2 + \frac{I_3}{R}\bar{C}_J\right)\cos\lambda_r x \sin\mu_s\theta \cos\lambda_m x \sin\mu_n\theta\\
& + \left(\frac{\gamma}{R}\right)^2 \left(\bar{B}_I I_2 + \frac{I_3}{R}\bar{D}_I\right)\left(\bar{B}_J I_2 + \frac{I_3}{R}\bar{D}_J\right)\sin\lambda_r x \cos\mu_s\theta \sin\lambda_m x \cos\mu_n\theta\\
& + \gamma^2 \sin\lambda_r x \sin\mu_s\theta \sin\lambda_m x \sin\mu_n\theta \Bigg\} \mathrm{d}\theta\, \mathrm{d}x
\end{aligned}
$$

$$= \begin{cases} \dfrac{\alpha L}{4}(A_I^* A_J^* + B_I^* B_J^* + C_I^* C_J^* + D_I^* D_J^* + E_I^* E_J^*) & \text{if } I = J \\ 0 & \text{if } I \neq J \end{cases} \tag{23}$$

$$\mathbf{M}_{IJ} = \mathbf{M}_{IJ}\omega_J^2 \tag{24}$$

$$\mathbf{Q}_{IJ} = -\gamma I_1 R^2 \lambda_m \int_0^L \int_0^\alpha \frac{\partial}{\partial x}(\eta_s \cos \lambda_m x \sin \mu_n \theta) \sin \lambda_r x \sin \mu_s \theta \, \mathrm{d}\theta \, \mathrm{d}x$$

$$= \begin{cases} -\dfrac{\alpha L}{4}\gamma I_1 R^2 \lambda_r \lambda_m \eta_s & \text{if } I = J \\ 0 & \text{if } I \neq J \end{cases} \tag{25}$$

where

$$A_k^* = \gamma\left(I_1 \bar{A}_k + \frac{I_2}{R}\bar{C}_k\right)$$

$$B_k^* = \gamma\left(I_1 \bar{B}_k + \frac{I_2}{R}\bar{D}_k\right)$$

$$C_k^* = \frac{\gamma}{R}\left(I_2 \bar{A}_k + \frac{I_3}{R}\bar{C}_k\right)$$

$$D_k^* = \frac{\gamma}{R}\left(I_2 \bar{B}_k + \frac{I_3}{R}\bar{D}_k\right)$$

$$E_k^* = \gamma I_1 \tag{26}$$

and $k = 1, 2, 3, 4, \ldots, N$.

3. Stability analysis

Equation (20) is in the form of a second-order differential equation with periodic coefficients of the Mathieu–Hill type. Using the method presented by Bolotin (1964), the regions of unstable solutions are separated by periodic solutions having period T and $2T$ with $T = (2\pi/P)$. The solutions with period $2T$ are of greater practical importance as the widths of these unstable regions are usually larger than those associated with solutions having period T. As a first approximation the periodic solutions with period $2T$ can be sought in the form

$$\mathbf{q} = \mathbf{f}\sin\frac{Pt}{2} + \mathbf{g}\cos\frac{Pt}{2} \tag{27}$$

where $\mathbf{f}$ and $\mathbf{g}$ are arbitrary vectors.

Substituting eqn (27) into eqn (20) and equating the coefficients of the $\sin(Pt/2)$ and $\cos(Pt/2)$

Table 1
First four unstable regions for a panel of $b/R = 0.5$, $L/R = 2$ and under tensile loading of $\eta_0 = 1/2\eta_{cr}$

	Pt. of origin p			Angle subtended Θ		
	CST	FSDT	% diff	CST	FSDT	% diff
$h/R = 0.03$						
1st unstable reg (1,1)	0.7650871	0.7605915	0.59106	0.0256951	0.0258446	0.58149
2nd unstable reg (2,1)	1.0722443	1.0664572	0.54265	0.0726175	0.0729988	0.52507
3rd unstable reg (3,1)	1.5076184	1.4988417	0.58557	0.1162854	0.1169408	0.56358
4th unstable reg (4,1)	1.9975838	1.9832372	0.72339	0.1567566	0.1578453	0.69448
$h/R = 0.04$						
1st unstable reg (1,1)	0.9976844	0.9870142	1.08105	0.0263148	0.0265958	1.06781
2nd unstable reg (2,1)	1.3374792	1.3235779	1.05028	0.0777726	0.0785666	1.02091
3rd unstable reg (3,1)	1.8313471	1.8102993	1.16268	0.1277765	0.1292115	1.12310
4th unstable reg (4,1)	2.4111464	2.3769167	1.44009	0.1732664	0.1756690	1.38666
$h/R = 0.05$						
1st unstable reg (1,1)	1.2308019	1.2100794	1.71249	0.0266880	0.0271407	1.69633
2nd unstable reg (2,1)	1.6062721	1.5790699	1.72267	0.0810604	0.0824241	1.68235
3rd unstable reg (3,1)	2.1621062	2.1209467	1.94062	0.1354157	0.1379647	1.88239
4th unstable reg (4,1)	2.8345409	2.7679303	2.40651	0.1843507	0.1886388	2.32605

terms, a set of linear homogeneous algebraic equations in terms of $\mathbf{f}$ and $\mathbf{g}$ can be obtained. The conditions for non-trivial solutions are given by

$$\det\left[\begin{pmatrix} -\frac{1}{4}P^2\mathbf{M}_{IJ}+\mathbf{K}_{IJ}-\frac{1}{2}\mathbf{Q}_{IJ} & 0 \\ 0 & -\frac{1}{4}P^2\mathbf{M}_{IJ}+\mathbf{K}_{IJ}+\frac{1}{2}\mathbf{Q}_{IJ} \end{pmatrix}\right] = 0. \tag{28}$$

Instead of solving the above nonlinear geometric equations for P, the above expression can be rearranged to the standard form of a generalized eigenvalue problem

$$\det\left[\begin{pmatrix} \mathbf{K}_{IJ}-\frac{1}{2}\mathbf{Q}_{IJ} & \mathbf{0} \\ \mathbf{0} & \mathbf{K}_{IJ}+\frac{1}{2}\mathbf{Q}_{IJ} \end{pmatrix} - P^2\begin{pmatrix} \frac{1}{4}\mathbf{M}_{IJ} & \mathbf{0} \\ \mathbf{0} & \frac{1}{4}\mathbf{M}_{IJ} \end{pmatrix}\right] = 0 \tag{29}$$

where $\mathbf{0}$ is a $5N^2 \times 5N^2$ null matrix. The generalized eigenvalues P^2 of the above generalized eigenvalue problem define the boundaries between the stable and unstable regions and can be computed easily using any commercially available eigenvalue package.

4. Numerical results and discussion

The dynamic instability regions for the first-order parametric resonances of a shell panel under combined static and periodic axial loads are presented in Tables 1 and 2 and Figs 3 and 4. The non-dimensional excitation frequency parameter p is defined as

Table 2
First four unstable regions for a panel of $b/R = 0.5$, $L/R = 2$ and under compressive loading of $\eta_0 = 1/2\eta_{cr}$

	Pt. of origin p			Angle subtended Θ		
	CST	FSDT	% diff	CST	FSDT	% diff
$h/R = 0.03$						
1st unstable reg (1,1)	0.6532618	0.6483488	0.75777	0.0300034	0.0302256	0.74075
2nd unstable reg (2,1)	0.7182320	0.7110948	1.00370	0.1062933	0.1072842	0.93224
3rd unstable reg (3,1)	0.9171988	0.9060940	1.22557	0.1852367	0.1872843	1.10540
4th unstable reg (4,1)	1.1957598	1.1776127	1.54101	0.2528890	0.2563688	1.37601
$h/R = 0.04$						
1st unstable reg (1,1)	0.8854011	0.8739775	1.30707	0.0296026	0.0299832	1.28582
2nd unstable reg (2,1)	0.9715799	0.9549933	1.73684	0.1057441	0.1074819	1.64343
3rd unstable reg (3,1)	1.2023632	1.1760791	2.23489	0.1903083	0.1942196	2.05521
4th unstable reg (4,1)	1.5495172	1.5063851	2.86329	0.2626528	0.2694866	2.60184
$h/R = 0.05$						
1st unstable reg (1,1)	1.1183180	1.0964077	1.99837	0.0293425	0.0299214	1.97281
2nd unstable reg (2,1)	1.2346733	1.2030459	2.62894	0.1045971	0.1072303	2.51747
3rd unstable reg (3,1)	1.5135089	1.4632239	3.43659	0.1904003	0.1965104	3.20906
4th unstable reg (4,1)	1.9419439	1.8595201	4.43253	0.2639889	0.2747844	4.08938

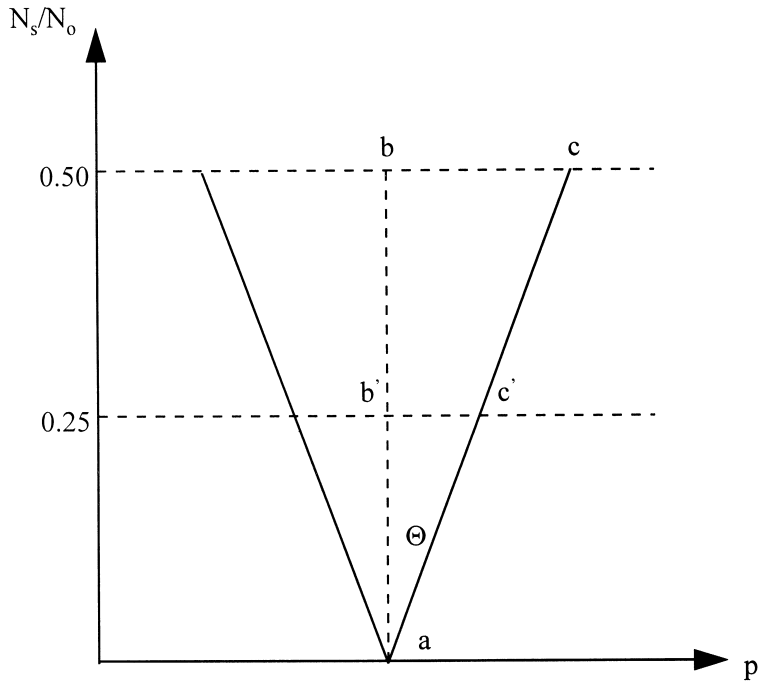

Fig. 2. An unstable region in the η_s/η_0-p plane.

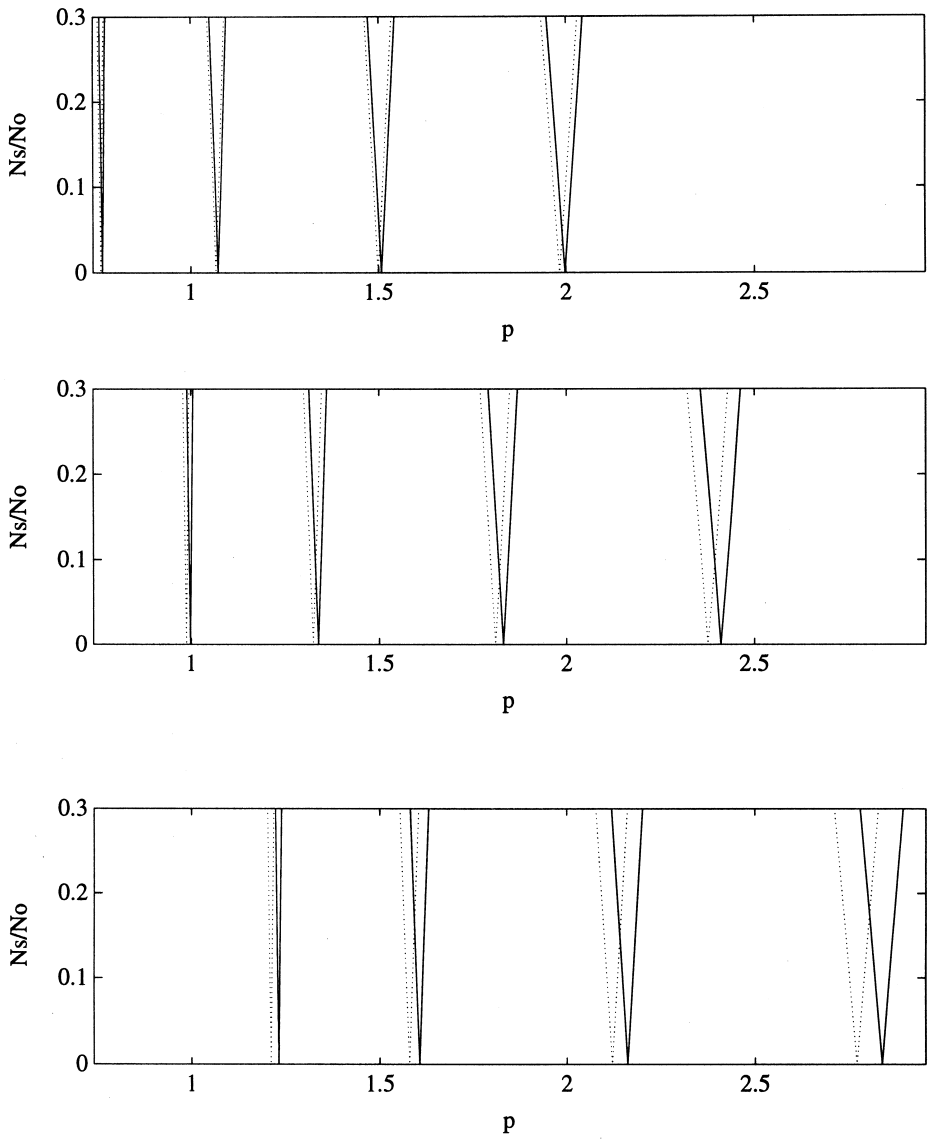

Fig. 3. First four unstable regions for a panel of $b/R = 0.5$, $L/R = 2$ and under tensile loading of $\eta_0 = 1/2\eta_{cr}$. —, CST, . . . , FSDT. Upper diagram, $h/R = 0.03$. Middle diagram, $h/R = 0.04$. Lower diagram, $h/R = 0.05$.

$$p = RP\sqrt{\frac{\rho(1-\nu^2)}{E}}. \tag{30}$$

Each unstable region is bounded by two curves originating from a common point from the p-axis with $\eta_s = 0$. The two curves appear at first glance to be straight lines but are in fact two very slight 'outward' curving plots. For the sake of tabular presentation, the angle subtended, Θ, is

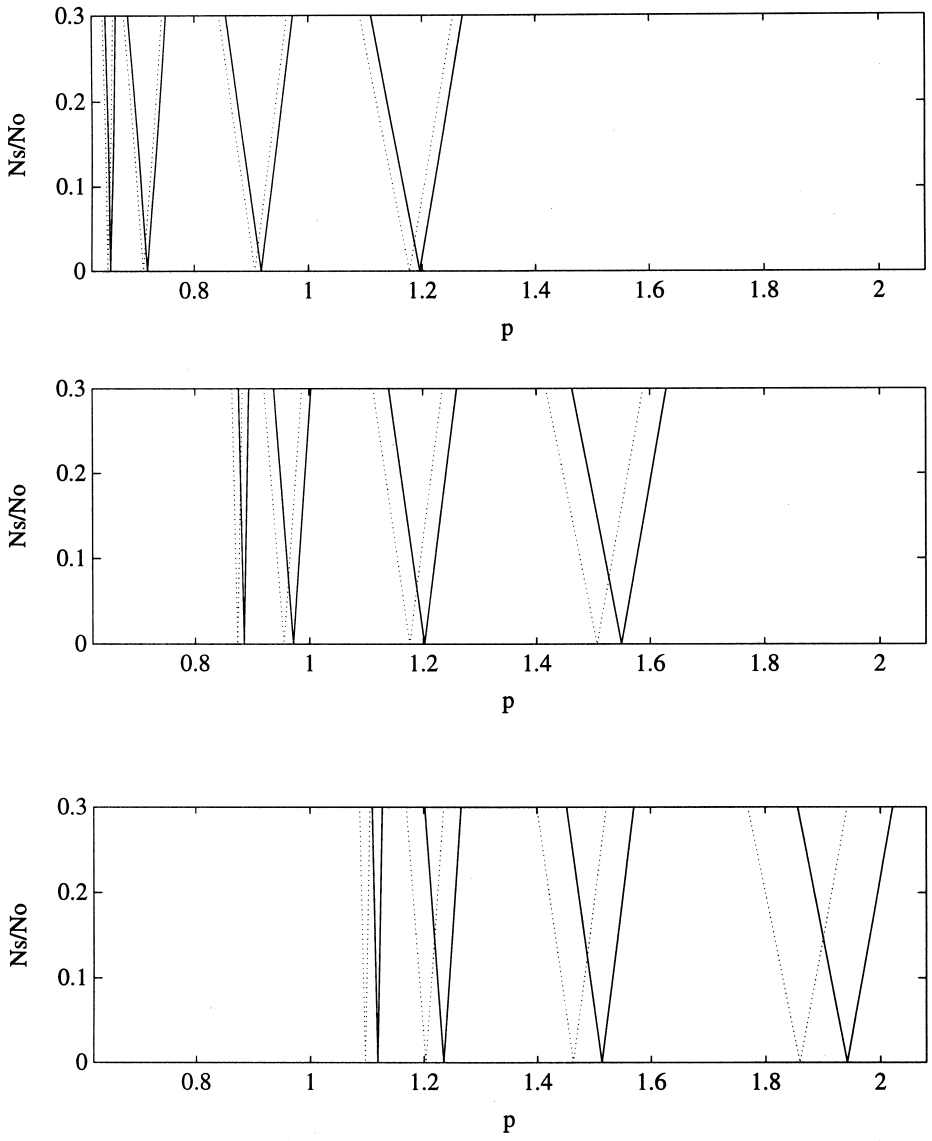

Fig. 4. First four unstable regions for a panel of $b/R = 0.5$, $L/R = 2$ and under compressive loading of $\eta_0 = -1/2\eta_{cr}$. —, CST, . . . , FSDT. Upper diagram, $h/R = 0.03$. Middle diagram, $h/R = 0.04$. Lower diagram, $h/R = 0.05$.

introduced. It is calculated based on the arctangent of the right-angled triangle, *abc*, obtained by halving the whole unstable region as shown in Fig. 2. This angle gives a good measure of the size of the unstable region as calculations done with the smaller similar triangle, $ab'c'$ (see Fig. 2), are within 0.02%.

For the results presented here, $\nu = 0.3$, $L/R = 2$ and $k_4 = k_5 = 5/6$. Tables 1 and 2 are the tabular

results of Figs 3 and 4, respectively. The values of η_0 are chosen to be in terms of η_{cr} which is the critical buckling load of a simply-supported circular cylindrical shell subjected to static compressive axial load and is given by

$$\eta_{cr} = N_{cr}\left(\frac{1-v^2}{Eh}\right) \tag{31}$$

where N_{cr} as given in Timoshenko and Gere (1961) is

$$N_{cr} = \frac{Eh^2}{[3(1-v^2)]^{1/2}R} \tag{32}$$

and if v is taken to be 0.3, then

$$n_{cr} = 0.5507\frac{h}{R}. \tag{33}$$

The results presented are restricted to thin, shallow panels of thickness ratio $h/R \leqslant 0.05$ and shallowness ratio $b/R \leqslant 0.5$ due to the limitations of the approximations on the curvature terms made in Donnell's theory. This is to ensure that the errors in the CST results are due to neglect of transverse shear effects rather than Donnell-type approximations on the curvature terms. The results presented also exclude those for circumferential wave number $n > 4$ due to the limitation of Donnell's equations to the higher modes in short to moderate length shell panels. The magnitude of the axial loading used is $\eta_0 = 1/2\eta_{cr}$.

Table 1 and Fig 3 examine the instability regions generated by the two theorems for panels of different thickness to radius ratios h/R under tensile loadings. From Table 1 and Fig. 3, comparing the results obtained by CST and FSDT, it is observed that the points of origins of the unstable regions are generally lower and the sizes of the unstable regions generally larger when FSDT is used. Thus the inclusion of transverse shear and rotary inertia effects in the FSDT are of importance as it generates more conservative results. It is also observed that for higher thickness ratios, the points of origin are higher. This can be expected as the points of origin which corresponds to twice the natural frequencies of the panels are expected to increase with increased stiffness associated with the increased thickness. It is also observed that the sizes of the unstable regions increased as the thickness of the panel was increased. The percentage differences between the CST results and FSDT results increased as the thickness of the panel was increased, giving more and more conservative results. This is expected as the inclusion of transverse shear and rotary inertias will have more effect on a thicker panel in making it less stiff than on a thinner shell. It is also interesting to note that the percentage increase in the sizes of the unstable regions using FSDT corresponds closely to the percentage decrease in the magnitude of the points of origin when using CST.

Table 2 and Fig. 4 presents the corresponding results for compressive loadings. Here again, the points of origins of the unstable regions are generally lower and the sizes of the unstable regions generally larger when FSDT is used. An interesting observation here is that the discrepancy between the CST and FSDT results are more pronounced for the cases with compressive loadings than those with tensile loadings. When comparing corresponding results for tensile and compressive loadings, it is generally observed that the panels under compressive loadings have lower points of origins and larger sizes of unstable regions. This observation holds for both CST and FSDT.

5. Conclusion

The dynamic stability of simply-supported, isotropic cylindrical panels under combined static and periodic axial forces has been investigated using the generalized Donnell's shell theory. A system of Mathieu–Hill equations were obtained via a normal-mode expansion and the parametric resonance response was analyzed using Bolotin's method. First order shear deformation (FSDT) as well as classical shell theory (CST) were used and results were compared. The inclusion of transverse shear and rotary inertias in the FSDT generated more conservative results when compared with results from the CST especially for thicker panels. The sizes of the unstable regions were observed to increase as the thickness of the panel was increased.

References

Bert, C.W., Chen, T.L.C., 1978. Effect of shear deformation on vibration of anti-symmetric angle-ply laminated rectangular plates. Int. J. Solids Structures 14, 465–473.

Bert, C.W., Kumar, M., 1982. Vibration of cylindrical shells of bimodulus composite materials. J. of Sound Vibr. 81, 107–121.

Blevins, R.D., 1981. Natural frequencies of shallow cylindrically curved panels. J. Sound Vibr. 75, 145–149.

Bolotin, V.V., 1964. The Dynamic Stability of Elastic Systems. Holden-Day, San Francisco.

Carrera, E., 1991. The effects of shear deformation and curvature on buckling and vibrations of cross-ply laminated composite shells. J. Sound Vibr. 150, 405–433.

Donnell, L.H., 1933. Stability of Thin Walled Tubes Under Torsion. NACA Report No. 479.

Flugge, W., 1962. Stresses in Shells. Springer-Verlag, Berlin.

Gulati, S.T., Essenberg, F., 1967. Effects of anisotropy in axisymmetric cylindrical shells. J. Appl. Mech. 34, 650–666.

Koumousis, V.K., Armenakas, A.E., 1984. Free vibration of noncircular cylindrical panels with simply supported curved edges. J. Engng Mech. 110, 810–827.

Leissa, A.W., Lee, J.K., Wang, A.J., 1981. Vibrations of cantilevered shallow cylindrical shells of rectangular planform. J. Sound Vibr. 78, 311–328.

Love, A.E.H., 1944. Treatise on the Mathematical Theory of Elasticity. Dover, New York.

Moorthy, J., Reddy, J.N., Plaut, R.H., 1990. Parametric instability of laminated composite plates with transverse shear deformation. Int. J. Solids Structures 26, 801–811.

Muc, A., 1989. Transverse shear effects in stability problems of laminated shallow shells. Composite Structures 12, 171–180.

Nosier, A. and Reddy, J.N., 1991. Vibration and stability analysis of cross-ply laminated circular cylindrical shells. J. Sound Vibr. 157, 139–159.

Palazotto, A.N., Linnemann, P.E., 1991. Vibration and buckling characteristics of composite cylindrical panels incorporating the effects of higher order shear theory. Int. J. Solids Structures 28, 341–361.

Reddy, J.N., 1984. Exact solutions of moderately thick laminated shells. J. Engng Mech. 110, 794–809.

Reddy, J.N. 1996. Mechanics of Laminated Composite Plates—Theory and Analysis. CRC Press, Florida.

Sanders, J.L., 1959. An Improved First Approximation Theory for Thin Shells. NASA Report NASA-TRR24.

Soldatos, K.P., Hadjigeoriou, V.P., 1990. Three-dimensional solution of the free vibration problem of homogeneous isotropic cylindrical shells and panels. J. Sound Vibr. 137, 369–384.

Timoshenko, S.P., Gere, J.M., 1961. Theory of Elastic Stability. McGraw-Hill, New York.

Vijayaraghavan, A., Evan-Iwanowski, R.M., 1967. Parametric instability of circular cylindrical shells. J. Appl. Mech. 31, 985–900.

Webster, J.J., 1968. Free vibrations of rectangular curved panels. Int. J. Mech. Sci. 10, 571–582.

Yao, J.C., 1965. Nonlinear elastic buckling and parametric excitation of a cylinder under axial loads. J. Appl. Mech. 29, 109–115.

Zukas, J.A., Vinson, J.R., 1971. Laminated transversely isotropic cylindrical shells. J. Appl. Mech. 38, 400–407.